January and July climate simulations over the SADC region using the limited-area model DARLAM

FA Engelbrecht[1*], CJ deW Rautenbach[1], JL McGregor[2] and JJ Katzfey[2]

[1] *LRAM, Department of Geography, Geoinformatics and Meteorology, Faculty of Natural and Agricultural Sciences, University of Pretoria, Pretoria 0002, South Africa*

[2] *CSIRO Atmospheric Research, PB1 Aspendale, 3195, Victoria, Australia*

Abstract

High-resolution climate simulations of near-surface variables are presented for January and July over the Southern African Developing Countries (SADC) region using the CSIRO Division of Atmospheric Research Limited-Area Model (DARLAM) nested within a General Circulation Model (GCM). The model domain includes tropical (north and south of the equator) and sub-tropical (Southern Africa) regions. Objective measures of skill are used to assess the quality of model simulations, and the performance of the model is verified over various subregions of the model domain. South of the tropics, DARLAM fields are not only superior to those produced by the GCM, but also compare well with mesoscale observations. This is particularly true for the spatial distribution of rainfall and screen temperature simulations. DARLAM, however, severely over-estimates rainfall totals over regions of steep orography.

Introduction

Mesoscale atmospheric circulation systems and surface forcing have an important influence on the climate of sub-Saharan Africa. For example, the steep escarpment of southern and eastern South Africa induces the occurrence of large spatial differences in rainfall totals over relatively short distances (Engelbrecht and Rautenbach, 2000). In central Africa, mesoscale forcing over Lake Victoria results in what is probably the highest frequency of thunderstorms in the world (Asnani, 1993), while exceptionally strong sea-breeze circulation cells are responsible for the dominant winds along the coastlines of Madagascar and Namibia (Jackson, 1954).

On the synoptic scale, most general circulation models (GCMs) succeed to adequately simulate the main characteristics of the general circulation over Southern Africa (Joubert, 1997). However, at this point in time computational requirements prevent GCMs from performing climate simulations at mesoscale resolutions of a few kilometres to about 100 km (Giorgi and Mearns, 1991; McGregor et al., 1993a). A technique known as nested climate modelling (NCM) has therefore been introduced as a computationally feasible alternative to obtain high-resolution climate simulations over limited areas of the earth. NCM involves the nesting of a high-resolution limited-area model (LAM) within the grid of a GCM over the area of interest. With a relatively finer horizontal resolution, the LAM may then succeed to capture some of the mesoscale properties of the atmospheric circulation.

The Australian Commonwealth Scientific and Industrial Research Organisation (CSIRO) Division of Atmospheric Research Limited-Area Model (DARLAM) has been used for climate modelling experiments over many locations of the world at a variety of horizontal and vertical resolutions. Most simulations have been performed by nesting DARLAM either within the CSIRO-9 GCM, or within observational analyses, over Australian domains. A one-way nesting technique was employed in all the DARLAM simulations. In the one-way nesting approach the LAM simulations are not allowed to interact with and influence the driving GCM analyses. The earliest simulations were for perpetual January conditions (McGregor and Walsh, 1991; 1993). Subsequently, multiple January and July simulations have been performed (Walsh and McGregor, 1995), followed more recently by full seasonally varying simulations of up to 20 years duration (McGregor, 1999). The latest mesoscale climate simulations were nested for 140 years within a CSIRO-9 GCM transient simulation. In these simulations DARLAM utilised horizontal grid resolutions of 125 km and 60 km with 9 levels in the vertical (McGregor, 1999). In general it was found that the LAM simulations, especially at higher latitudes, were superior to the associated GCM simulations and compared well with regional observations over the Australian continent.

Joubert et al. (1999) used DARLAM to simulate the January climate over a domain covering Africa south of the equator. Using a one-way nesting procedure, lateral boundary and initial conditions were supplied by the CSIRO-9 GCM. The experiment consisted of 20 January ensemble members nested individually at 125 km x 125 km resolution within the GCM. It was found that DARLAM captured the spatial pattern of observed rainfall and inter-annual rainfall variability over the region as a whole more accurately than the GCM. Over the steep eastern escarpment of South Africa, DARLAM produced more rainfall than the GCM and significantly more than observed. In general, DARLAM produced a more accurate and detailed simulation of the January climate over Southern Africa than the coarse resolution GCM. This is largely attributed to the fact that regional geographical features, which influence the climate of Southern Africa, are more clearly resolved by the 125 km x 125 km LAM resolution (Joubert et al., 1999).

This paper describes results from a new initiative where even higher resolution (60 km x 60 km horizontal grid resolution) DARLAM climate simulations have been performed using a domain of 100 x 100 grid points that covers the entire area (Fig. 1) of the Southern African Developing Countries (SADC). The size of the domain is not only larger than in any previously performed high-resolution climate simulations over Southern Africa, but also has

* To whom all correspondence should be addressed.
☎ 012 420-4943; fax 012 420 3284; e-mail: fengelbr@postino.up.ac.za
Received 25 March 2002; accepted in revised form 8 July 2002.

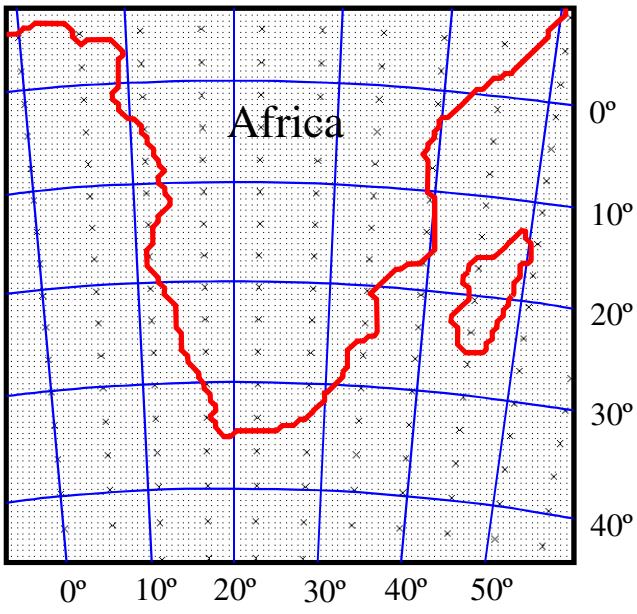

Figure 1
DARLAM domain used for simulations over the SADC region. The 60 km x 60 km spaced model grid points on a Lambert conformal projection are indicated by dots. Gaussian grid points of the R21 CSIRO-9 GCM are indicated by crosses.

the finest horizontal and vertical resolution ever used. A one-way nesting procedure has been followed to produce model-simulated climate fields for January and July. Results from a long seasonal-varying simulation of the CSIRO-9 R21 GCM were used to supply DARLAM with the necessary information at its lateral boundaries. Since the DARLAM domain covers the entire SADC region, an important feature of the simulations is the inclusion of extensive regions north and south of the equator in the model domain (Fig. 1). One might expect that DARLAM should perform better over mid-latitude than tropical regions. Weather systems generally move more slowly over tropical regions and internal quasi-stationary systems, that are not influenced by the boundary forcing, may evolve within the nested model domain making simulations over the tropics more complex (Walsh and McGregor, 1995). It is worthwhile to note that large regions over the entire Southern Africa are influenced by tropical systems.

The aim of the paper is to explore the possibilities and limitations of the NCM technique to produce high-resolution climate simulations over the SADC region. A qualitative and quantitative comparison is made between the DARLAM / GCM climate simulations of mean sea-level pressure (MSLP), screen temperature, near-surface wind and rainfall for January and July and the associated observed fields. Of particular interest is the extent to which the higher resolution of the LAM contributes to improved climate simulations of near-surface conditions over the subcontinent.

Model description

The CSIRO-9 Mk 2 GCM

The CSIRO-9 Mk 2 GCM (Gordon and O'Farrell, 1997) used here is a coupled atmosphere-ocean climate model with R21 spectral resolution that utilises an east-west grid of 64 equally spaced longitudes and a pole to equator grid of 28 unevenly spaced Gaussian latitudes. The model integrates the flux formulation of the primitive equations (Gordon, 1981) forward in time over 9 σ-levels in the vertical (Rautenbach, 1999). The flux formulation ensures that both energy and mass are conserved during model integrations - a property that is vital when a GCM is used for multi-annual climate simulations (Gordon, 1981; 1983). Time integration is performed by means of a semi-implicit leapfrog scheme. Apart from the dynamics, the CSIRO-9 GCM contains a comprehensive range of physical processes including radiation and precipitation (McGregor et al., 1993b).

DARLAM

DARLAM has been developed for use in both short-term mesoscale studies and longer-term climate simulation experiments. The model is a two-time-level, semi-implicit, hydrostatic primitive equations model. It uses an Arakawa staggered C-grid and semi-Lagrangian horizontal advection with bi-cubic spatial interpolation. The model utilises a Lambert conformal projection and has 18 σ-levels in the vertical. DARLAM employs physical parameterisations similar to those used in the CSIRO-9 GCM, which include a modified version of the Arakawa (1972) cumulus convection scheme, a six-layer soil moisture scheme and the Geophysical Fluid Dynamics Laboratory (GFDL) diurnally-varying parameterisation for long-wave and short-wave radiation (Fels and Schwarzkopf, 1975; Schwarzkopf and Fels, 1991). It also uses a stability-dependent boundary-layer, based upon the Monin-Obukhov similarity theory (Louis, 1979). Soil temperatures are calculated using a six- layer model with a zero-flux condition at the bottom. The LAM and GCM use a different treatment for the evaluation of available soil moisture ("α-method" for the GCM and the "β-method" for DARLAM following the terminology of Kondo et al. (1990)).

Experimental design

A one-way NCM technique is employed with lateral boundary conditions supplied every 12 h by the CSIRO-9 GCM. At each time-step the outermost DARLAM boundary grid points are relaxed toward interpolated GCM values. The nesting procedure of Davies (1976) is used, but with exponentially decreasing weights. Initial atmospheric conditions (including soil moisture) are supplied by the forcing GCM, and sea-surface temperatures (SSTs) prescribed every 12 h by the GCM linearly interpolated in time.

In this study nine separate 30 d model simulations have been performed for both January and July. The ensemble average of these nine simulations constitutes the model climate for each month. It should be noted that the averaged nine simulations are not sufficient to truly represent the definition of the term climate, but serves as a demonstration of the possibility of using the NCM technique for regional climatic studies. The 30 d simulations incorporated both diurnal and seasonally varying radiation, but were initialised separately with output fields taken from the CSIRO-9 GCM. No vertical-mode initialisation was performed and no spin-up period was included for the moisture cycle to reach equilibrium. Similar experiments over the Australian region indicated that the spin-up process has a negligible effect on the DARLAM climate (Walsh and McGregor, 1995). For surface pressure and soil temperatures, the boundary fields were adjusted to compensate for differences between the interpolated higher resolution DARLAM and smoothed GCM orographies.

In the experiments the LAM utilised a horizontal resolution of 60 km x 60 km with 18 σ-levels in the vertical. A time-step of 15 min was used. The DARLAM simulations were performed at the Laboratory for Research in Atmospheric Modelling (LRAM), at

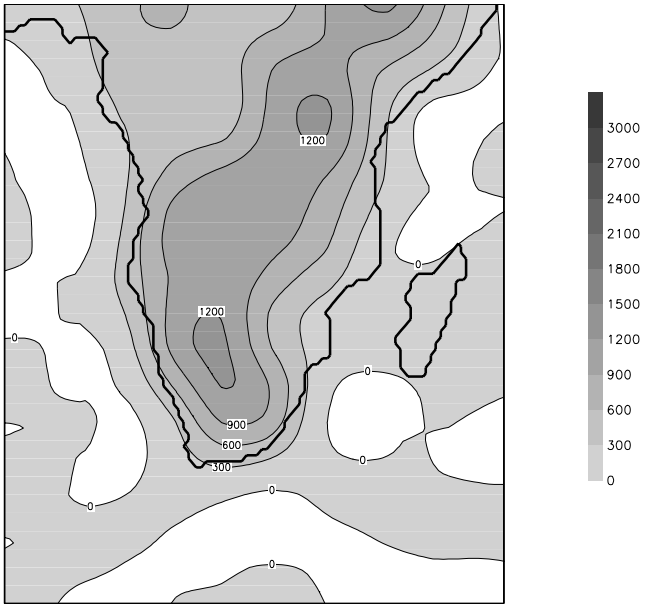

Figure 2a
CSIRO-9 GCM representation of orography at R21 spectral resolution over the SADC region. The contour interval is 300 m. Note the smoothed elevation over land and negative elevation over the oceans.

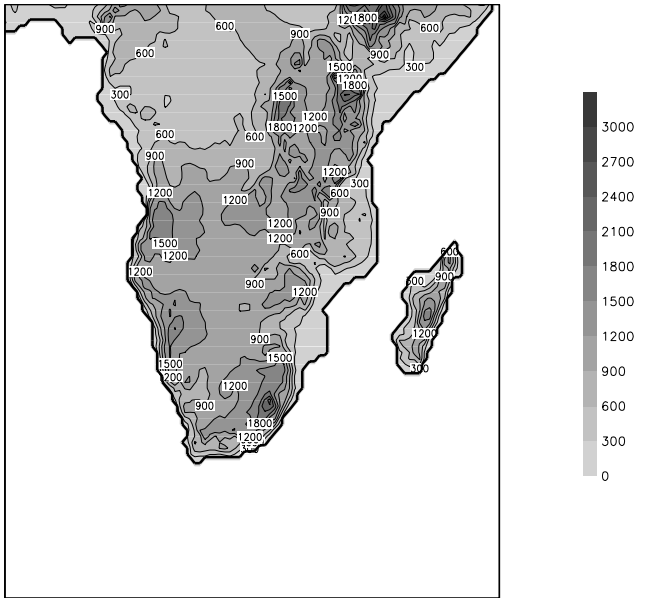

Figure 2b
DARLAM representation of orography at 60 km grid point resolution over the SADC region. The contour interval is 300 m.

the University of Pretoria, on a Pentium III workstation with two 550 MHz processors. It took approximately 11 min (CPU time) to simulate a model day at the specified model resolutions.

Observational data and model verification methods

The results discussed here involve the comparison to observations of simulations by the CSIRO-9 GCM and DARLAM. It is therefore important to have statistically rigorous means to evaluate whether a particular field of the LAM is superior to that of the GCM. Following Walsh and McGregor (1995) a standard statistical measure, namely the pattern correlation, is used to assess the quality of model simulations.

The pattern correlation (ρ) of two spatial grid fields at a specific time is the correlation of a series of grid points x_i from the one field with the corresponding grid points o_i from the other field; i ranges between 1 and N, where N is the number of grid points in the model domain):

$$\rho = \frac{\sum (x_i - \bar{x})(o_i - \bar{o})}{\left[\sum (x_i - \bar{x})^2\right]^{1/2}\left[\sum (o_i - \bar{o})^2\right]^{1/2}} \qquad (1)$$

Here $\bar{x}$ and $\bar{o}$ are the domain averages of x_i and o_i respectively. In this study, pattern correlations have been calculated between LAM and GCM fields, and between both models and observations. Observations and GCM output fields were both interpolated to the DARLAM grid. A bilinear interpolation technique was used, which is adequate given the smooth nature of the monthly averaged fields (Walsh and McGregor, 1995). Summations in Eq. (1) were performed over all grid points, excluding the outermost three rows at the LAM boundaries.

The assessment of the quality of model simulations over the SADC region and adjacent oceans is severely hampered by the lack of reliable, high-resolution observed data. For the oceans, over which there is a complete lack of reliable observations, no high-resolution observed data sets exist. The National Centre for Environmental Prediction (NCEP) reanalysis data (Kalnay et al., 1996) is suitable for qualitative model verification, but the relatively low spatial resolution (2.5ºx 2.5º) of NCEP data (compared to the 60 km x 60 km grid resolution data of DARLAM) renders the NCEP data unsuitable for quantitative model verification over either ocean or land. In this paper, model output of MSLP and near-surface winds are graphically compared with NCEP reanalysis data. In addition, pattern correlations have been calculated, in order to compare GCM MSLP fields with those of the LAM.

Statistical analysis of model output against observations is restricted to the sub-continent only. Here, model screen temperatures and rainfall have been verified against the 1961 to 1990 observed climate data set (New et al., 1999) of the Climate Research Unit (CRU). Much of the spatial and temporal characteristics of a range of surface climate variables over Southern Africa can be observed in the 0.5ºx 0.5º CRU data. Over many areas, however, the fields still remain quite smooth due to their inherent dependence on relatively low-resolution data from point observations. The verification of the results produced by DARLAM is therefore far from ideal.

Model orographies

The interior of South Africa is characterised by an elevated plateau with altitudes in excess of 1 000 m. Maximum altitudes of higher than 3 500 m occur along the South African eastern escarpment, as well as over tropical East Africa. The coastal margins along the east and south-east coast of Southern Africa are narrow and marked by steep orographic gradients. The R21 spectral resolution of the CSIRO-9 GCM uses a significantly smoothed orography as lower altitude boundary (Fig. 2a). The plateau is narrow and maximum altitudes are under-estimated by as much as 2 500 m. Orographic gradients along the escarpment are also very gentle. The orography of Madagascar is poorly resolved and extremely smooth over the entire island. Islands such as Mauritius and La Reunion are not captured at all. The spectral method requires that the surface

orography is spectrally fitted to a wave resolution of R21. The initial observed orography data field has a 1°x1° resolution. This field was spatially averaged in the 64 x 56 global Gaussian grid boxes of the CSIRO-9 GCM, and then spectrally resynthesized to an R21 resolution (McGregor et al., 1993b). A consequence of this procedure is that non-zero or even negative sea elevations might occur in the model orography (Fig. 2). This might be attributed to the so-called Gibbs phenomenon (McGregor et al., 1993b).

With a finer horizontal resolution of 60 km x 60 km, DARLAM provides a more detailed representation of actual regional orographic features over Southern Africa (Fig. 2b). More realistic maximum elevations occur over the escarpment of south-eastern South Africa (in excess of 2 400 m above mean sea-level) and Tropical East Africa (in excess of 3 000 m above mean sea-level). Features such as steep orographic gradients along the southern African escarpment and the Namibian highlands are well captured. The eastern mountain ranges of Madagascar are more obvious and realistic. Even smaller islands such as Mauritius, La Reunion and the Comoros are visible in the DARLAM orography field (not shown). This represents a significant improvement relative to the GCM orography.

Results and discussion

The tropical problem

When using a one-way NCM to produce regional climate simulations, it is normally assumed that the development of atmospheric systems within the LAM domain is constrained by boundary condition forcing. Although it is expected that the LAM should add significant mesoscale detail compared to that of the GCM, it should also be consistent with the synoptic scale driving analyses of the GCM.

The boundary conditions also provide a means of removing possible flow inconsistencies between the driving analyses of the GCM and the internal response of the LAM. This is particularly appropriate for higher-latitudinal regions where weather systems regularly sweep through the LAM domain (Errico and Baumhefner, 1987). It is therefore expected that the one-way NCM technique should perform better in mid-latitudinal regions than in the tropics. At tropical latitudes, where weather patterns move more slowly than in the mid-latitudes, quasi-stationary systems that do not depend on GCM forcing may develop within the LAM domain (McGregor, 1997). The LAM solution may eventually diverge from the driving analyses on the synoptic scale, which may represent a physical inconsistency. This inconsistency may be called the "tropical problem" (McGregor, 1997). The one-way NCM approach therefore has some theoretical limitations, especially in the tropics. Nevertheless, Walsh and McGregor (1995) successfully performed a number of tropical climate simulations over the Australian region using a model domain that included extensive regions north and south of the equator.

In this paper the LAM domain includes large areas north and south of the equator (Fig. 1). In an attempt to quantify the tropical problem, the model domain was sub-divided into various latitudinal bands. The location of the bands and the number of LAM grid points in each band are listed in Table 1. For reasons that will become obvious soon, land and ocean grid points are considered separately.

Figure 3a depicts January MSLP pattern correlations between GCM and LAM simulations for grid points in the various latitudinal bands. It is obvious that the pattern correlation between the GCM and LAM simulations is significantly lower over the strong tropical region than over regions to the south. This is most probably as a result of the tropical problem and suggests that LAM simulation

TABLE 1
Latitudinal bands and number of grid points located in each band

Latitudinal band in model domain		Total number of grid points	Number of ocean points	Number of land points
All points		8836	5381	3455
Strong tropics	*<10°S*	2726	996	1730
Tropics	*10°S to 20°S*	1694	780	914
Sub-tropics	*20°S to 30°S*	1713	1065	648
Mid-latitudes	*>30°S*	2703	2540	163

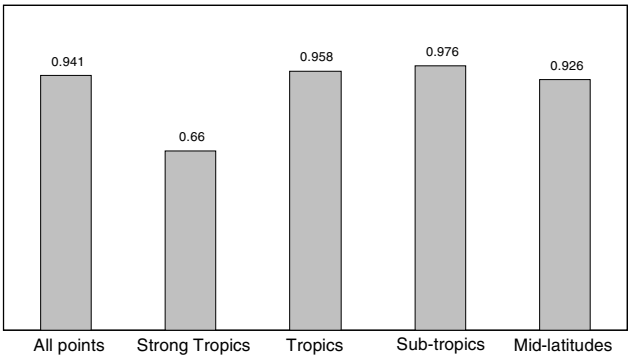

Figure 3a
January Mean Sea-Level Pressure (MSLP) pattern correlations between the GCM and DARLAM for the various latitudinal bands defined in Table 1

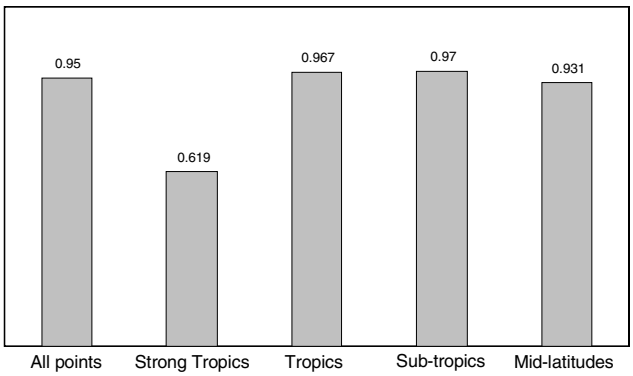

Figure 3b
January MSLP pattern correlations as in Fig. 3a, but for ocean points only

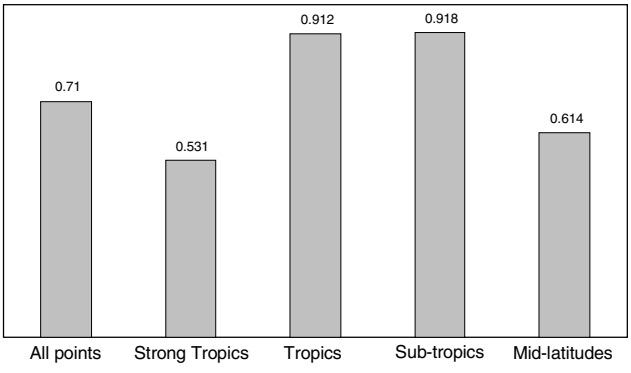

Figure 3c
January MSLP pattern correlations as in Fig. 3a but for land points only

over the tropics should be interpreted with caution. Higher pattern correlations for regions to the south indicate the model flows are more consistent there, as a result of the strong boundary forcing from the GCM. Figures 3b and 3c are similar to Fig. 3a, but for ocean and land points, respectively. A comparison of Figs. 3b and 3c reveals that, irrespective of the latitudinal band, pattern correlations are always higher over the ocean than over the continent. Over continental areas the high-resolution orographic features of the LAM may enhance the simulation of mesoscale circulation patterns not captured by the GCM. This will result in lower pattern correlations, particularly of near-surface variables over land points compared to ocean points. Near-surface temperature pattern correlations between the two models (not shown) are qualitatively similar to those for MSLP. Pattern correlations between MSLP and near-surface temperatures for July (not shown) are also in qualitative agreement with those of January.

Mean sea-level pressure

Climate patterns of observed MSLP (from NCEP data) over the SADC region and adjacent oceans are illustrated in Figs. 4.1a (January) and 4.1b (July). The January MSLP distribution over the SADC region is characterised by a deep continental low-pressure system (heat low) located over Botswana and Namibia and two well-defined anticyclones over the oceans adjacent to the subcontinent (Fig. 4.1a). A well-developed meridional pressure gradient is present to the south of South Africa where the pressure drops toward the circumpolar trough. Lower pressures occur over the tropical subcontinent, emphasising the presence of the southern extension of the Inter-Tropical Convergence Zone (ITCZ). The relatively higher MSLP recorded over south-eastern South Africa and eastern Madagascar are the result of migrating high-pressure systems that frequently ridge to the south of the African continent during summer.

During the austral winter the observed oceanic anticyclones intensify and shift northward (Fig. 4.1b). At the same time a well-developed high-pressure belt develops over the subcontinent. The meridional pressure gradient to the south of South Africa increases as a result of the deeper circumpolar trough, causing westerly winds to intensify. Over tropical regions south of the equator pressures are generally higher in association with the northward propagation of the ITCZ during winter.

The semi-stationary low-pressure cell (a trough in July) present in the NCEP reanalysis field over the Mozambique channel (Figs. 4.1a and 4.1b) might be regarded as a giant lee low that originates downwind of the eastern Madagascar mountain range in the persistent easterly wind flow (wind vectors in Figs. 4.1a and 4.1b). The amplitude of this trough

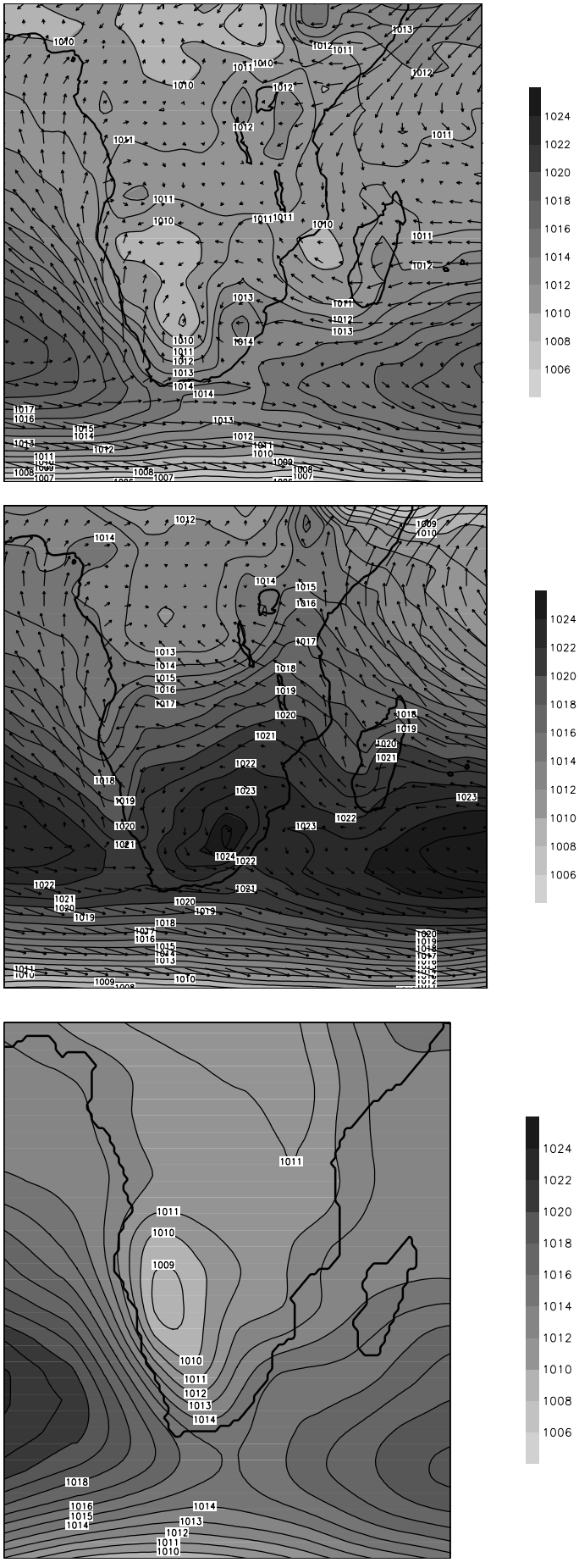

Figure 4.1a
Observed MSLP measured in hPa and near-surface wind vectors (at 10 m altitude) meassured in m·s^{-1} for January as obtained from a 40-year (1958 to 1998) NCEP reanalysis climatology. The contour interval is 1 hPa.

Figure 4.1b
Observed MSLP and near-surface wind vectors as in Fig. 4.1a, but for July

Figure 4.1c
MSLP in hPa for January as simulated by the CSIRO-9 GCM. The contour interval is 1 hPa

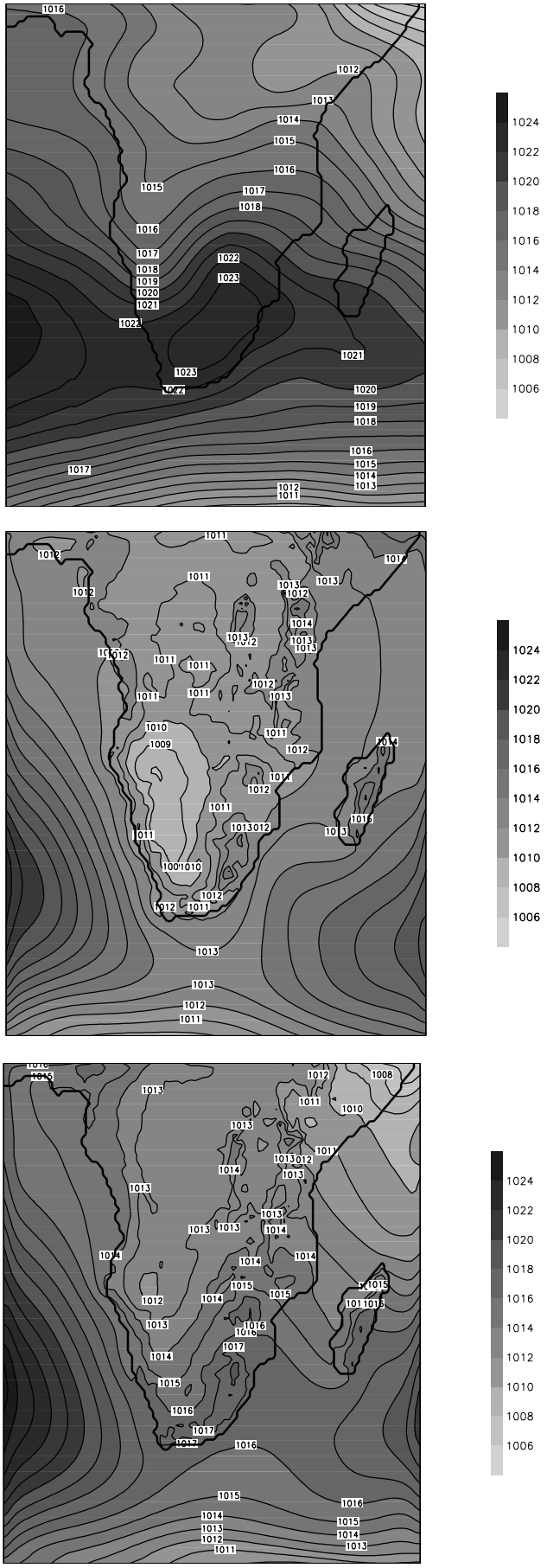

and its southward extent decreases in the austral winter (Fig. 4.1b). The increased amplitude and greater southward extent during January is likely to result from the observed southward shift of the south-easterly trade wind regime during the austral summer, in association with the usual simultaneous occurrence of relative higher SSTs in the Mozambique channel.

In general, synoptic-scale features of the observed MSLP are adequately reproduced in the CSIRO-9 GCM simulations for January and July (Figs. 4.1c and 4.1d). In the January simulation (Fig. 4.1c), the low-pressure cell over Namibia and Botswana is located further to the north and west than observed, although the intensity of the cell is well simulated. The relative positions and meridional position of the oceanic anticyclones are well captured. The amplitudes of both these cells however, are overestimated. The meridional pressure gradient to the south of South Africa closely corresponds to the observed gradient. The GCM overestimates MSLP over tropical regions and fails to reproduce the presence of lower pressures in the Mozambique Channel where MSLP is overestimated by as much as 4 hPa. The GCM also fails to capture the pattern of relatively higher MSLP over the south-eastern part of South Africa and eastern Madagascar.

The CSIRO-9 GCM successfully simulates the observed northward shift and intensification of the subtropical anticyclones in July, as well as the tighter meridional pressure gradient associated with the deeper circumpolar trough (Fig. 4.1d). The simulation of amplitudes of the broader July MSLP pattern is weaker when compared to the simulation of January amplitudes. In particular, the intensity of the Indian Ocean high-pressure system is underestimated by more than 4hPa. As in the January simulations, the GCM generates higher than observed MSLPs over the tropical regions and again fails to simulate the trough in the Mozambique Channel. The GCM simulation however, does capture the higher pressures over tropical regions south of the equator (relative to January) implying that the model succeeds to simulate the northward displacement of the ITCZ during the austral winter.

Due to the GCM's forcing at the lateral boundaries of the LAM domain, the January and July MSLP patterns simulated by the two models are expected to be similar. The two model simulations indeed have much in common, especially over maritime regions where the influence of the higher resolution surface orography of the LAM is absent. The lower intensities of the two subtropical oceanic high-pressure systems, as simulated by DARLAM for January (Fig. 4.1e), are slightly more realistic than the GCM simulations (compare Figs. 4.1a, 4.1c and 4.1e). The DARLAM continental low over the western subcontinent is larger in extent and a little more realistic than found in GCM simulations. The low simulated by DARLAM also extends further to the south and east.

DARLAM simulations of MSLP over Southern Africa and Madagascar contain far more detail than the corresponding GCM simulations. DARLAM adequately simulates the observed pattern of high-pressure intrusion over the south-eastern parts of South Africa and Madagascar (compare Figs. 4.1a and 4.1e). This might be attributed to the high resolution orography in DARLAM which enables the model to capture low-level mass convergence along the

Figure 4.1d
MSLP as in Fig. 4.1c, but for July

Figure 4.1e
MSLP in hPa for January as simulated by DARLAM. The pressure contour interval is 1 hPa

Figure 4.1f
MSLP as in Fig. 4.1e, but for July

south-eastern escarpment of South Africa and Madagascar when high pressure systems ridge to the south of Africa. The GCM, with its smooth orography, fails to capture this pattern (compare Figs. 4.1c and 4.1a). Another notable feature of DARLAM is the simulation of the observed low in the Mozambique Channel. Altitudes in the DARLAM orography over Madagascar are in excess of 1 200 m (Fig. 2b), which is sufficient to induce the development of a gigantic lee low that is located downwind of the Madagascar mountain range. DARLAM, however, underestimates the intensity of the low. This low is not present in the GCM simulation - probably as a result of the smoothed orography (Fig. 2a).

Similar to the GCM simulations, July MSLP simulations by DARLAM (Fig. 4.1f) show an underestimation of the intensity of the Indian Ocean high-pressure system. Over tropical regions DARLAM simulates lower MSLPs than the GCM. This corresponds reasonably well to the observed pattern. DARLAM severely underestimates the intensity of the subtropical high-pressure belt over the African continent (by as much as 6 hPa), as well as the intensity of the meridional pressure gradient to the south of Africa. In this respect DARLAM simulations are inferior to the associated GCM simulations. Underestimation of the intensity of the high-pressure belt could be related to responses of the radiation scheme used in the model - an issue that needs to be investigated.

Near-surface wind patterns

The climatology of wind vectors from the NCEP reanalyses data at an altitude of 10 m is superimposed upon the MSLP in Figs. 4.1a (January) and 4.1b (July). The associated model simulated streamlines on the lowest model levels ($\sigma = 0.98$ for the GCM and $\sigma = 0.995$ for DARLAM) are illustrated in Figs. 4.2a and 4.2b (CSIRO-9 GCM) and 4.2c and 4.2d (DARLAM).

As noted above the CSIRO-9 GCM does not capture the observed low-level convergence in the Mozambique Channel that usually occurs during January in association with the low over the area (compare Figs. 4.1a and 4.2a).

Both DARLAM and the CSIRO-9 GCM reproduce the zone of convergence over the western parts of Southern Africa in January (Figs. 4.2a and 4.2c). The convergence is associated with the observed continental low that usually develops over Namibia and Botswana during the austral summer. However, over the central and eastern interior of South Africa, the CSIRO-9 GCM produces north-easterly flow (Fig. 4.2a) whilst DARLAM simulates a pronounced northerly to north-westerly flow (Fig. 4.2c). The NCEP reanalysis shows dominant easterly winds over this region with a tendency for northerly winds to prevail west of the escarpment. In this respect, it is also worthwhile to note that in reality the orography of Madagascar turns easterly to north-easterly flow, which prevails over the ocean to the east of the island in January, into easterly flow over the Mozambique Channel (Fig. 4.1a). DARLAM captures this phenomenon to some extent (Fig. 4.2c) but the CSIRO-9 GCM, with its smooth orography, persists with north-

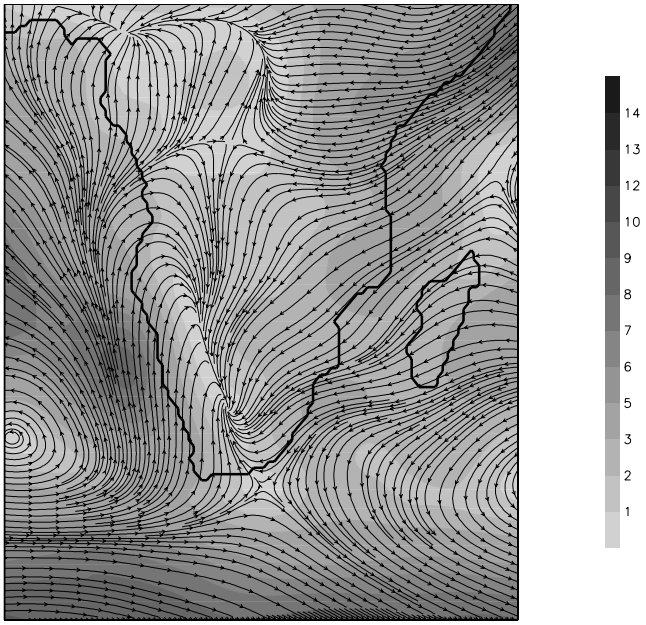

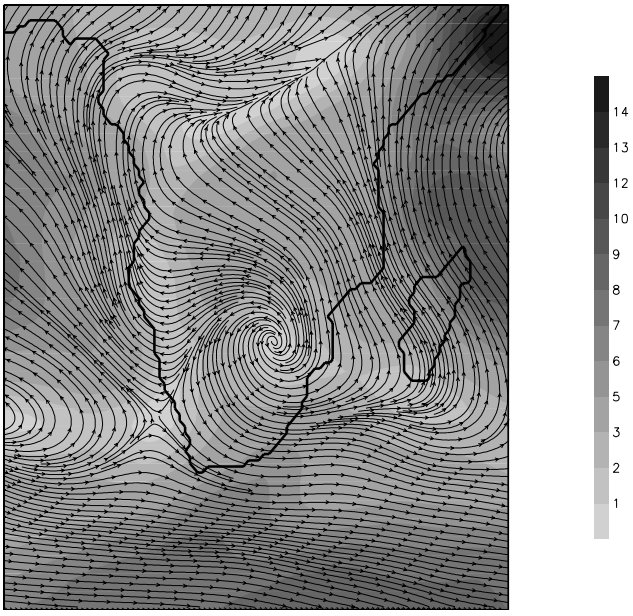

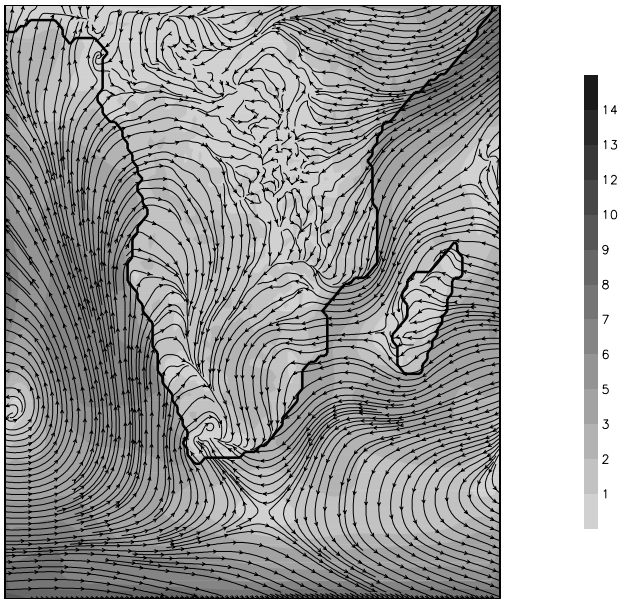

Figure 4.2a
Mean streamlines at the lowest model level (σ) in $m.s^{-1}$ for January as simulated by the CSIRO-9 GCM

Figure 4.2b
Mean streamlines as in Fig. 4.2a, but for July

Figure 4.2c
Mean streamlines at the lowest model level (σ) in $m \cdot s^{-1}$ for January as simulated by DARLAM

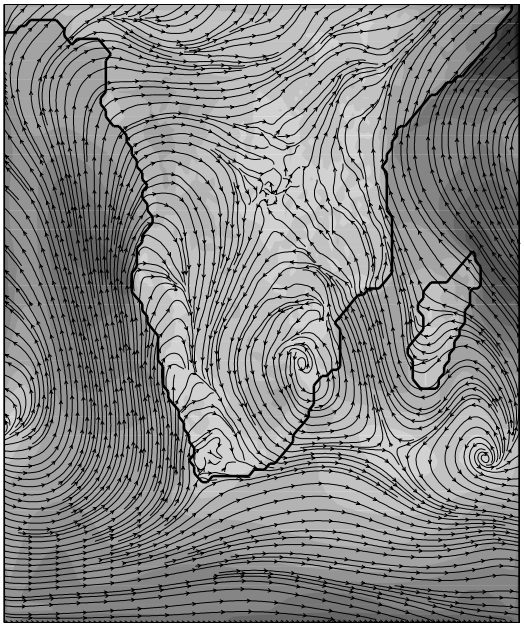

Figure 4.2d
Mean streamlines as in Fig. 4.2c but for July

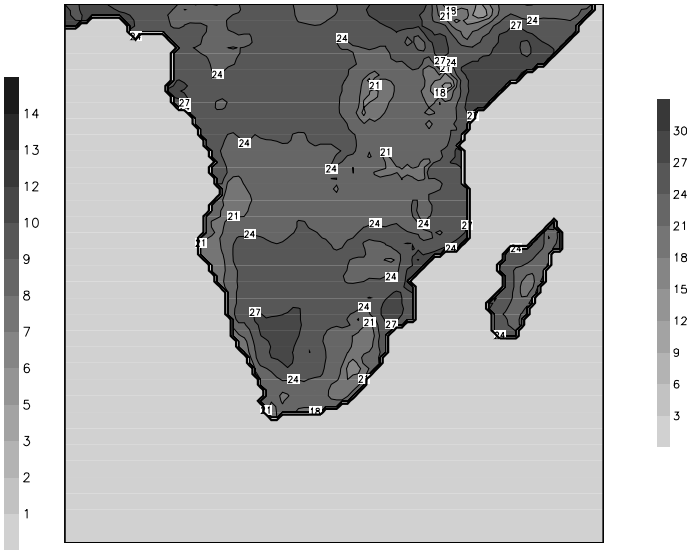

Figure 4.3a
Observed screen temperature climate (ºC) for January as obtained from the CRU climatology. The contour interval is 3ºC.

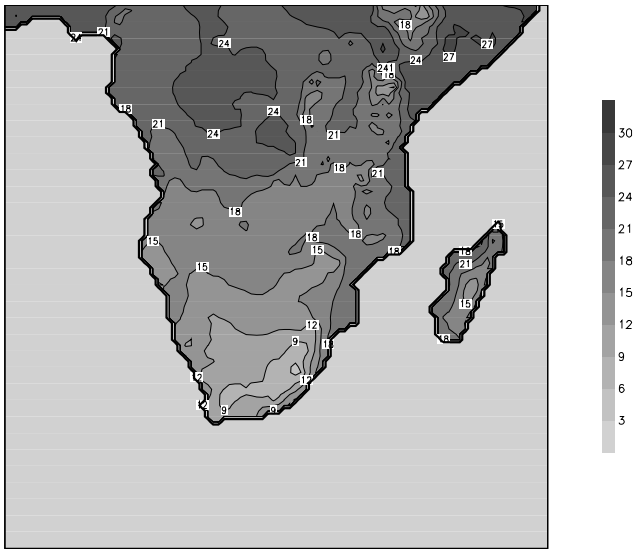

Figure 4.3b
Observed screen temperature as in Fig. 4.3a, but for July.

easterly flow over the Mozambique Channel and eventually also over the eastern parts of South Africa (Fig. 4.2a). In fact, south of 20ºS over the coast of Mozambique, south-easterly flow can be observed (Fig. 4.1a). DARLAM simulates easterly flow over this area (Fig. 4.2c) but the GCM persists with north-easterly streamlines (Fig. 4.2a).

Compared to the CSIRO-9 GCM, DARLAM simulates weaker low-level westerly flow to the south of Africa in both the January and July climatologies (Figs. 4.2a, 4.2b, 4.2c and 4.2d). The observed flow is generally stronger than simulated by either DARLAM or the CSIRO-9 GCM. The weaker DARLAM flow is more obvious in the July simulation when DARLAM also underestimates the meridional pressure gradient to the south of South Africa, as well as the intensity of the subtropical high pressure belt over the interior of South Africa (Fig. 4.1f).

For July, both models reproduce the observed winter offshore flow over the eastern parts of South Africa (Figs. 4.1b, 4.2b and 4.2d). The offshore flow is a result of counter-clockwise rotation in the subtropical high-pressure zonal belt over the region (Figs. 4.1b, 4.2d and 4.2f). Once again DARLAM improves on the GCM simulation by capturing the cyclonic flow around the trough that is situated over the western parts of Madagascar (Figs. 4.1b and 4.2d).

Screen and surface temperature

Figures 4.3a (January) and 4.3b (July) provide some detail concerning the observed features of the average screen temperature distribution over the SADC region and adjacent oceans (CRU climatology). During January and especially July a well-defined meridional temperature gradient is present over the region. Although not shown here, temperatures are lower over the Atlantic Ocean (where the cold Benguela ocean current is associated with upwelling along the western coastline of Southern Africa) than over the Indian Ocean. In the Mozambique Channel, where the warm Agulhus ocean current flows southward, higher temperatures likewise intrude far to the south. For the same latitudinal value, the screen temperature is generally higher over the east coast compared to the west coast, due to the modifying effect of the mentioned ocean currents on coastal climate. This is especially true during the austral winter (Fig. 4.3b) when the relative importance of surface forcing increases.

During January average screen temperature maximams in excess of 27ºC are observed in tropical East Africa, the western interior of South Africa, Botswana, Mozambique and Southern Nigeria (Fig. 4.3a). In both the January and July fields, the important modifying influence of orography on screen temperature over the region is well illustrated. Lower isotherms from the south extend northward over the high altitude region of south-eastern South Africa. The steep escarpment along this region is also associated with steep temperature gradients, especially during the austral winter (Fig. 4.3b) when maximum insolation shifts northwards and orographic effects become more profound. The eastern Madagascar mountain range has a similar effect on temperature distribution

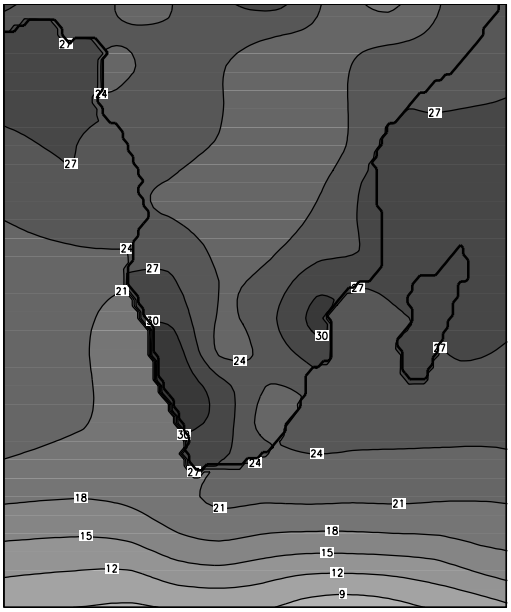

Figure 4.3c
Surface temperature climate (ºC) for January as simulated by the CSIRO-9 GCM. The contour interval is 3ºC.

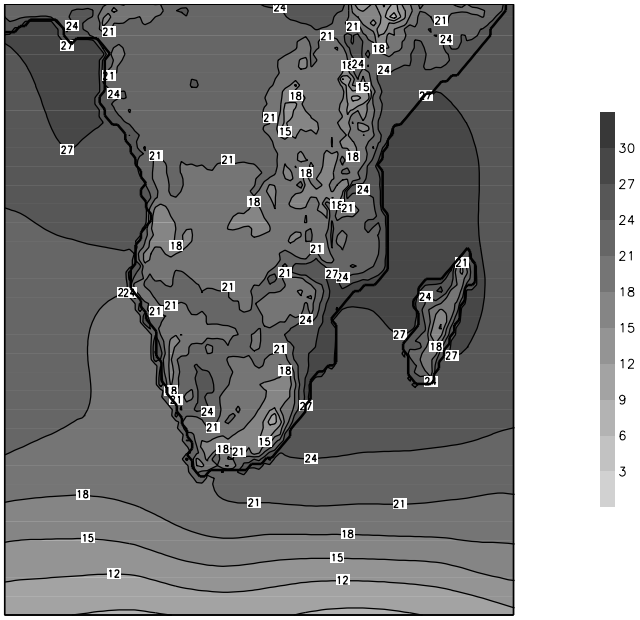

Figure 4.3e
Screen temperature climate (ºC) for January as simulated by DARLAM. The contour interval is 3 ºC.

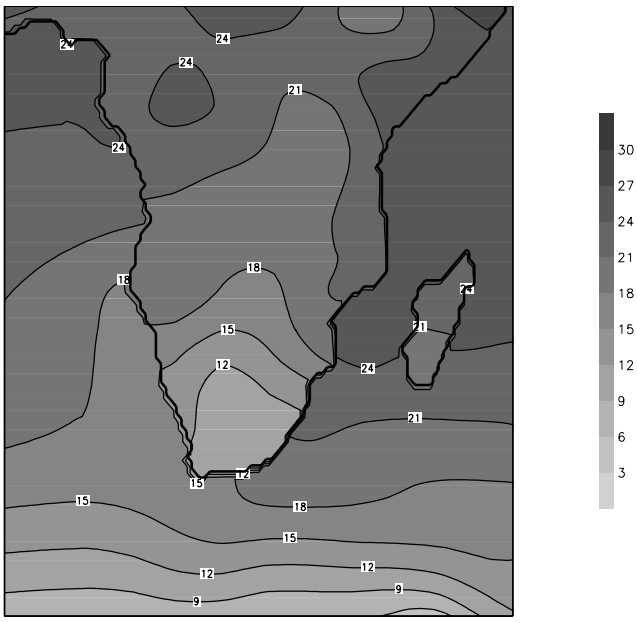

Figure 4.3d
Surface temperature climate as in Fig. 4.3c, but for July

over the island (Figs. 4.3a and 4.3b). Another prominent feature of the observed temperature distribution is the relatively high temperatures that occur in the low-lying Zambezi River valley in Mozambique (Figs. 4.3a and 4.3b).

When comparing CSIRO-9 GCM and DARLAM simulated temperatures it is essential to keep in mind that the GCM simulations represent surface temperatures, whilst DARLAM and CRU data are screen height air temperatures. This explains why the CSIRO-9 GCM temperatures are on average a degree or two higher than the observed and LAM simulated fields. In general, simulations from the two models have specific similarities, but there are also some major differences. DARLAM contains a more detailed representation of the land/ocean boundary. This is especially noticeable along the western coastline, where the change in screen temperature is more abrupt in the LAM simulations (Figs. 4.3e and 4.3f) compared to the surface temperature of the CSIRO-9 GCM (Figs. 4.3c and 4.3d). Both models capture the observed meridional temperature gradient, the northward intruding lower temperatures along the western coastline and the southward extending higher temperatures along the eastern coastline.

Compared to the CSIRO-9 GCM simulations, DARLAM temperature patterns are in general closer to the associated observed patterns over the land-masses. DARLAM reproduces the observed January temperature maximams over the western interior of South Africa, Botswana, Tropical East Africa, Mozambique and Southern Nigeria (Fig. 4.3e). Note that DARLAM underestimates these temperature maximams by a degree or two. The CSIRO-9 GCM, however, spuriously simulates temperature maximams for January (Fig. 4.3c) in a broad band over Namibia at the lee side of the smoothed GCM model plateau (Fig. 2a). The GCM also fails to simulate the temperature maximum observed over tropical East Africa during January. This may be attributed to the fact that the low-altitude Great East African Valley with its associated higher temperatures is not embedded in the smoothed GCM orography (Fig. 2a). The higher resolution DARLAM orography does resolve this feature (Figs. 4.3e and 4.3f) resulting in a significantly improved simulation of screen temperature over the region (compare Figs. 4.3c and 4.3e to 4.3a). DARLAM also succeeds in capturing the relatively high temperatures observed in the Zambezi River valley (Figs. 4.3e and 4.3f), a feature not present in the GCM simulations. Both DARLAM and the CSIRO-9 GCM underestimate temperatures over Mozambique in January.

Both models capture the observed intrusion of lower isotherms over the south-eastern interior of South Africa that usually occur during January and July. Over this region DARLAM July temperature simulations (Fig. 4.3f) compare well with observations (Fig. 4.3b). DARLAM however, severely overestimates the

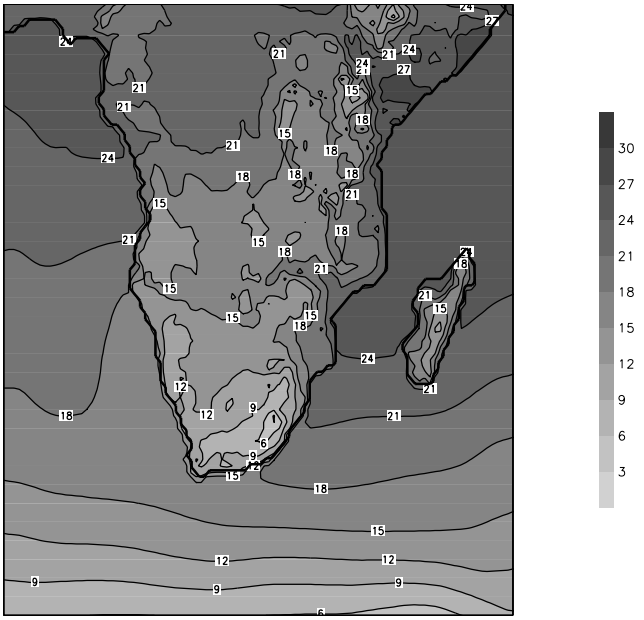

Figure 4.3f
Screen temperature climate as in Fig. 4.3e, but for July

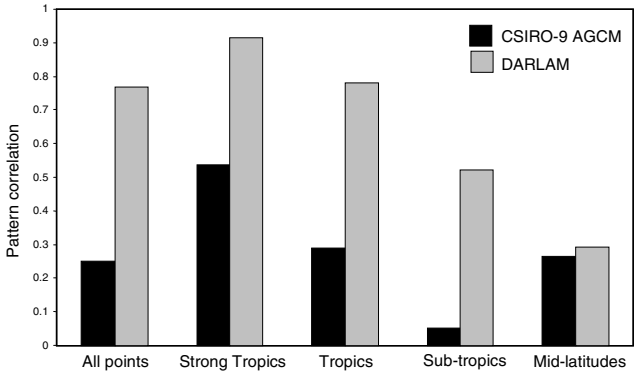

Figure 4.4a
January near-surface temperature pattern correlations between the GCM and CRU data and DARLAM and CRU data for land points over various latitudinal bands

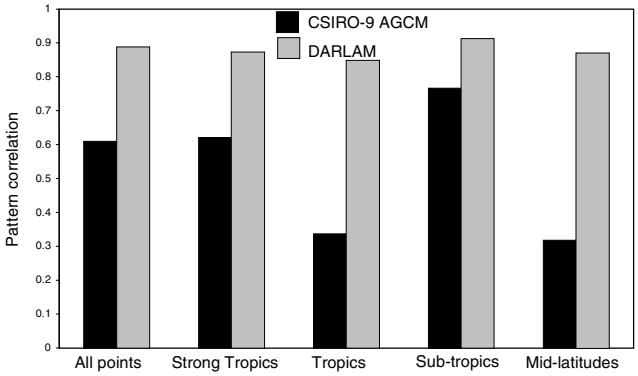

Figure 4.4b
Near-surface temperature pattern correlations as in Fig. 4.4a, but for July

occurrence of lower temperatures over the south-eastern interior of South Africa in January. Analysis of DARLAM rainfall simulations (discussed in the next section) indicates that DARLAM severely overestimates rainfall totals over this region. The overestimation of rainfall may be responsible for the underestimation of screen temperature as a result of excessive evaporative cooling at the model surface.

In both the January and July simulations DARLAM successfully captures the observed west-east temperature gradient over Madagascar (Figs. 4.3e and 4.3f), a feature that does not occur in the corresponding GCM simulations (Figs. 4.3c and 4.3d). As an air mass in the dominant easterly flow over Madagascar descends on the lee side of the mountain range, it will warm adiabatically to produce higher screen temperatures over the western parts of Madagascar. It seems that the adiabatic heating is adequately reproduced in DARLAM simulations, while the CSIRO-9 GCM with its smoothed orography fails to simulate this process satisfactorily.

Figure 4.4a shows pattern correlations between the GCM and CRU data and DARLAM and CRU data for January over the various latitudinal bands defined in Table 1. Pattern correlations between the LAM and CRU data are significantly higher compared to the correlations between the GCM and CRU data. The figure illustrates quantitatively how the LAM uses its high-resolution orography to simulate successfully the complex spatial distribution pattern of screen temperature over the region. During the austral winter, the LAM again produces significantly superior pattern correlations for temperature than the GCM (Fig. 4.4b). It is interesting to note that pattern correlations between the LAM and CRU data over the strong tropical region seems to be just as high as correlations calculated further to the south. This result may imply that the LAM model simulations over the strong tropical region have acceptable temperatures despite of the "tropical problem".

Rainfall

The rainfall climatology of the CRU data provides some indication of the observed rainfall distribution over the SADC region during January (Fig. 4.5a) and July (Fig. 4.5b). Interesting features of the observed data for January are the marked east-west gradient in rainfall totals that is present over South Africa, the band of relatively low rainfall present between 25ºS and 20ºS, and a band of relatively high rainfall that occurs between 15ºS and 10ºS (Fig. 4.5a). Arid conditions (with monthly rainfall totals below 20 mm) are present along the western coastline of South Africa, Namibia and Angola. Note that Madagascar experiences a rainfall maximum in the north-west and a rainfall minimum in the south-west during January (Fig. 4.5a).

During July, when the subtropical high-pressure belt establishes itself over the African subcontinent (Fig. 4.1b), observed rainfall totals over Southern Africa decrease significantly (Fig. 4.5b). The ITCZ shifts to the north, inducing higher rainfall over tropical regions north of the equator. A rainfall maximum occurs over Nigeria. Over Madagascar high rainfall totals are confined to the east of the escarpment. The southern coastline of South Africa and adjacent interior is influenced by cold fronts sweeping over the area from west to east causing winter rainfall (Fig. 4.5b).

The mean January rainfall distribution as simulated by the CSIRO-9 GCM is orientated in a north-west to south-east band across the subcontinent (Fig. 4.5c), which shows some correspondence to the observed east-west gradient (Fig. 4.5a). This distribution of simulated rainfall is most probably induced by the similar orientation of the smoothed GCM escarpment and plateau (Fig. 2a). The GCM captures neither the band of relatively lower

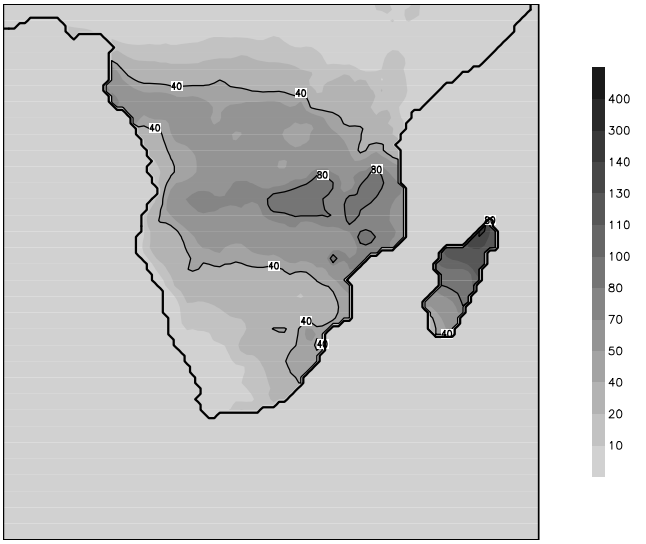

Figure 4.5a
Observed rainfall totals (mm) for January as obtained from the CRU climatology

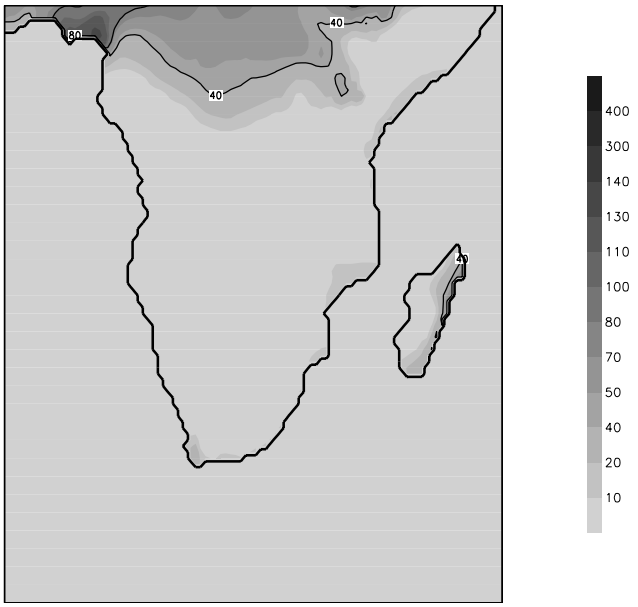

Figure 4.5b
Observed rainfall totals (mm) for July as obtained from the CRU climatology

rainfall between 25ºS and 20ºS nor the region of relatively higher rainfall totals between 15ºS and 10ºS. The GCM erroneously simulates an almost uniform rainfall distribution over Madagascar - once again due to it's smooth orography over this region (Fig. 2a). Note that over large regions of the domain the GCM simulates more than twice the amount of the observed rainfall.

The July CSIRO-9 GCM simulation apparently successfully captures the northward displacement of the ITCZ and subsequent drier conditions over Kenya and Somalia (Fig. 4.5d). The model adequately simulates the generally drier conditions that occur over the subcontinent during the austral winter. Rainfall totals increase over the south coast of South Africa, in harmony with the observed pattern (Fig. 4.5b).

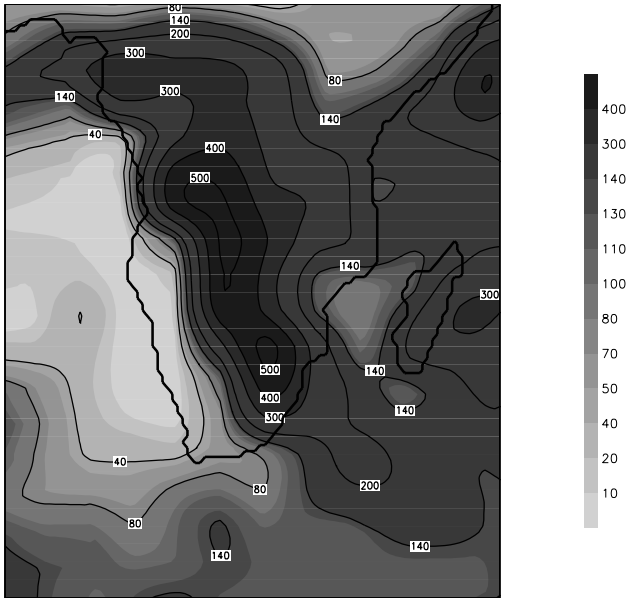

Figure 4.5c
Rainfall totals climatology (mm) for January as simulated by the CSIRO-9 GCM

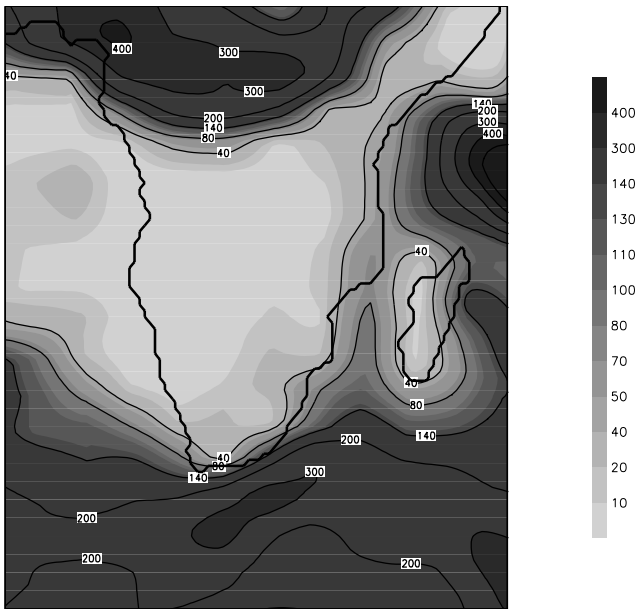

Figure 4.5d
Rainfall total climatology (mm) for July as simulated by the CSIRO-9 GCM

The mean January rainfall distribution as simulated by DARLAM (Fig. 4.5e) over South Africa is orientated more towards west-east than simulated by the CSIRO-9 GCM (Fig. 4.5c). This represents an improvement in the simulated rainfall pattern. DARLAM simulates the observed band of relatively higher rainfall between 15ºS and 10ºS. The LAM also simulates a band of relatively lower rainfall, although slightly north of the observed band (compare Figs. 4.5a and 4.4e). The LAM simulation of rainfall over Madagascar is quite detailed. The observed rainfall minimum in the south-west is captured, with an indication of increasing rainfall totals towards the north. More rainfall is simulated

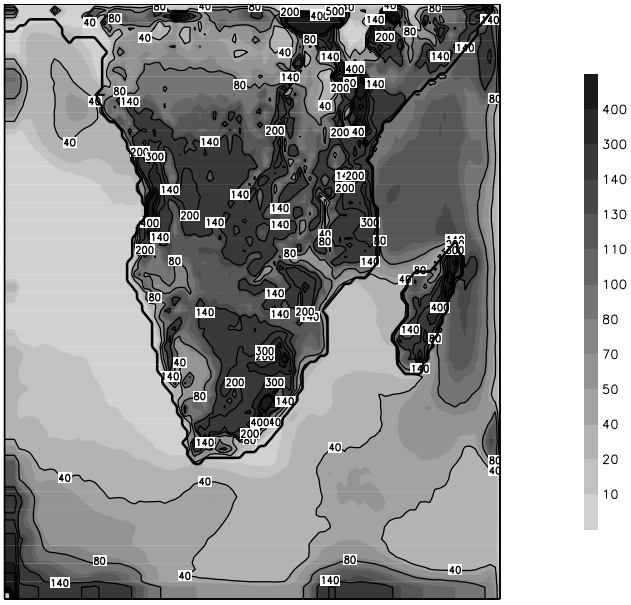

Figure 4.5e
Rainfall total climatology (mm) for January as simulated by DARLAM

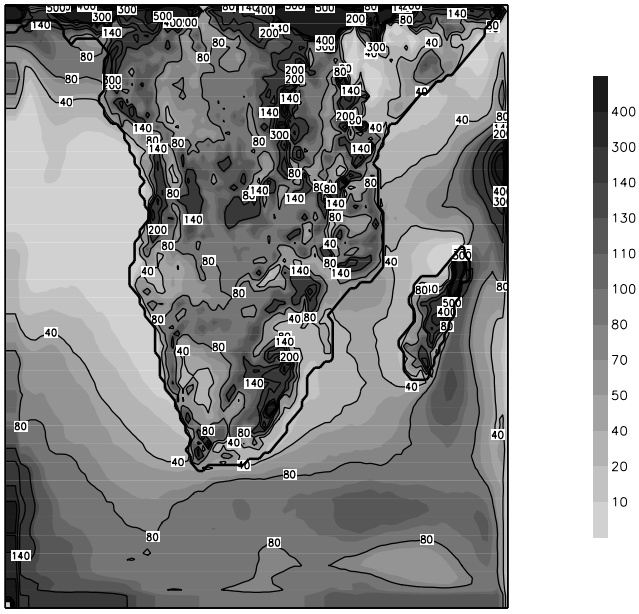

Figure 4.5f
Rainfall total climatology measured (mm) for July as simulated by DARLAM

to the east of the escarpment. This feature is most probably due to orographic uplift in the dominant easterly flow over the region. It is absent in the observed data, probably due to the inherently smooth nature of the CRU data set.

The northward displacement of high rainfall totals in the DARLAM simulation for July (Fig. 4.5f) suggests that the northward displacement of the ITCZ in the GCM simulation is adequately transferred to DARLAM through the lateral boundary forcing. Unfortunately DARLAM severely overestimates rainfall totals over the south-eastern escarpment of South Africa and the northern escarpment of Madagascar (Fig. 4.5f). The overestimation may be enhanced by the failure of DARLAM to capture the intensity of the subtropical high-pressure belt (and the associated subsidence) during the austral winter (Fig. 4.1f).

Along the escarpment, close to the mountains of Lesotho and the southern Drakensberg, DARLAM rainfall totals are up to six times the observed rainfall values for January (Fig. 4.6). During rainfall events over this area, the lower tropospheric flow is up-slope (perpendicular to the orographic obstacle) and the penetrating surface moisture is advected from the east where it originates from a ridging anticyclone (Joubert et al., 1999). It has been suggested earlier that DARLAM produces improved simulations (relative to the CSIRO-9 GCM) of the ridging high-pressures (and the associated low-level mass convergence) along the south-eastern escarpment of South Africa during January. This may partially explain why rainfall totals in this region are higher in the DARLAM simulations. It is highly interesting to note however, that DARLAM simulates the rainfall maximum over this area to the west of the model escarpment (Fig. 4.6). As pointed out earlier, simulated low-level winds over this area are from the north-west on average (Fig. 4.6), which may explain the simulation of high rainfall values west of the escarpment.

The mountain resonance effect, a phenomenon present in semi-Lagrangian model formulations, may sometimes contribute to the overestimation of mean vertical velocities and increased rainfall over steep orographic gradients (McGregor, 1997). Since the well-known Courant-Friedrichs-Lewy (CFL) criterion was satisfied in the present experiments, it is unlikely that the mountain resonance effect had an impact on the simulations. It is interesting to note however, that a vertical cross-section of orography and rainfall along approximately 30ºS (Fig. 4.7) does illustrate a strong correlation between DARLAM simulated rainfall maximums and elevation peaks. This suggests that the numerical methods used are indeed sensitive to steep model orography. In particular, terrain-following sigma-coordinate models such as DARLAM and the CSIRO-9 GCM can produce errors in the calculation of pressure-gradient forces near steep terrain. Finally it should be noted that the CSIRO-9 GCM also overestimates rainfall totals over the same region, although to a lesser extent than DARLAM. Thus it is also possible that spuriously large quantities of moisture are being transported by the forcing GCM to the eastern part of South Africa.

Conclusions

DARLAM generally provides a more accurate and detailed simulation of climate over the SADC region than the CSIRO-9 GCM. This may be attributed to the fact that orograpical features, which have a significant influence on the climate of the region, are more clearly resolved at the 60 km x 60 km resolution of the LAM than in the GCM. This is clearly illustrated by the improved LAM simulations of the spatial distribution pattern of screen temperature and rainfall over regions such as the south-eastern escarpment of South Africa, the Zambezi Valley and the Great East African Valley.

DARLAM's January climatology over the central parts of the model domain differs from that of the GCM and provides a better correspondence to observations. DARLAM adequately simulates the observed band of relatively higher rainfall between 15ºS and 10ºS. The LAM also simulates a band of relatively lower rainfall, although slightly north of the observed band. These features are absent in the GCM simulation. DARLAM successfully simulates the west-east gradient of rainfall over South Africa, instead of the north-east to south-west pattern of the GCM simulation. DARLAM

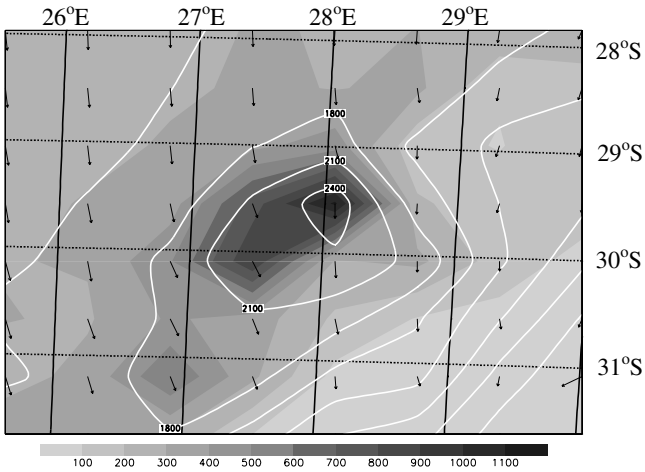

Figure 4.6
Rainfall totals (mm, shaded), low-level wind vectors ($m \cdot s^{-1}$, arrows) and orographical heights (m, contours) over the eastern escarpment region of South Africa

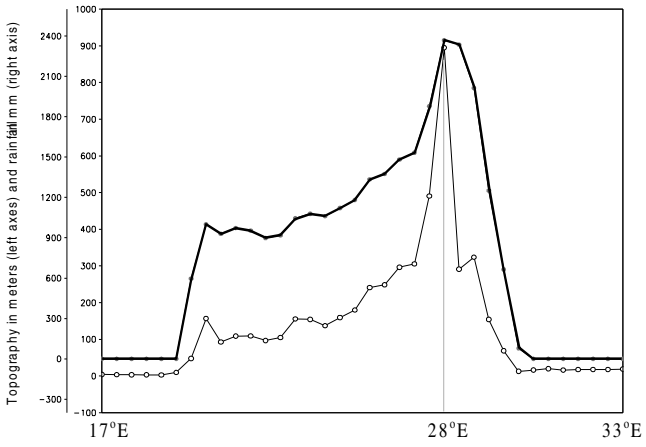

Figure 4.7
A vertical cross section of the DARLAM surface orography (m, thick line) with the January rainfall climatology measured (mm thin line) along the 30ºS latitude as simulated by DARLAM. Note the high rainfall totals along the eastern escarpment.

underestimates the intensity of the observed winter (July) subtropical high-pressure region over the subcontinent. This contributes to a severe overestimation of July rainfall totals over the south-eastern parts of South-Africa. In this respect the DARLAM simulation is inferior to the CSIRO-9 GCM simulation that successfully captures the intensification of the subtropical high during winter.

DARLAM simulations produce more than twice the amount of rainfall observed over regions with steep orographic gradients, such as the South African eastern escarpment. This result has also been noted in other atmospheric models over various regions of the world (Giorgi et al., 1994; McGregor and Walsh, 1994; Walsh and McGregor, 1995; Jenkins and Barron, 1997). Since the GCM also overestimates rainfall totals over this region, one may argue that more moisture is present in the LAM model domain due to spurious boundary forcing by the GCM. DARLAM successfully captures events of low-level mass convergence along the eastern escarpments of South Africa and Madagascar and the excess of moisture may result in simulations with excessive rainfall. Another possible contributing factor to the overestimation of rainfall may be inaccuracies in the calculation of pressure gradient forces near steep orography, which may be present in DARLAM's semi-Lagrangian dynamical formulation. The effectiveness of the numerical methods over the steep eastern escarpment of South Africa needs to be investigated in future experiments.

In a collaborative research between LRAM and CSIRO Atmospheric Research, ongoing experiments are planned to improve regional climate simulations over the SADC region. Encouraging preliminary results (lower rainfall totals and a rainfall maximum to the east of the escarpment) have been obtained with a new version of the DARLAM code. Case studies (using DARLAM) of significant rainfall events over the eastern escarpment of South Africa are planned for the near future. At the same time, the effect of different cumulus parameterisation schemes and the location of the eastern model boundary on the model simulations will be investigated. A cubic-conformal stretched grid GCM has also been introduced for climate simulations over the SADC region, with promising preliminary results. In a joint project, LRAM and the CSIRO Atmospheric Research are developing a non-hydrostatic version of this model. It is believed that non-hydrostatic dynamics will result in the improved simulation of vertical acceleration, and possibly improved rainfall totals over regions of steep orography.

Despite the problems that occur when simulating observed rainfall magnitudes over regions of steep orography, DARLAM provides a more accurate simulation of observed rainfall distribution, particularly in regions where the GCM's coarse resolution does not permit regional orographic features to be resolved. These preliminary simulations indicate that DARLAM is capable of simulating details on the regional scale with greater skill than the CSIRO-9 GCM.

Acknowledgements

The research in this paper forms part of a WRC funded project concerning LAM improvement over Southern Africa. The researchers would like to thank CSIRO Atmospheric Research in Australia for making DARLAM available to LRAM at the University of Pretoria, which enabled us to perform model simulations over the SADC region.

References

ARAKAWA A (1972) *Design of the UCLA General Circulation Model. Numerical Simulation of Weather and Climate.* Technical Report No. **7**. Department of Meteorology, University of California, Los Angeles.

ASNANI GC (1993) *Tropical Meteorology.* (Pune, India).

DAVIES HC (1976) A lateral boundary formulation for multi-level prediction models. *Quart. J. Roy. Meteorol. Soc.* **102** 405-418.

ENGELBRECHT FA and RAUTENBACH CJ deW (2000) Perspektief vir genestelde klimaatmodellering oor suidelike Afrika. *SA Tydskrif vir Wetenskap en Kuns* **19** 47-51.

ERRICO R and BAUMHEFNER D (1987) Predictability experiments using a high resolution limited-area model. *Mon.Weather.Rev*. **115** 408-418.

FELS SB and SCHWARZKOPF MD (1975) The simplified exchange approximation: a new method for radiative transfer. *J. Atmos. Sci*. **32** 1475-1488.

GIORGI F and MEARNS LO (1991) Approaches to the simulation of regional climate change: A review. *Rev. Geophys.* **29** 191-216.

GIORGI F, BRODEUR CS and BATES GT (1994) Regional climate change scenarios over the United States produced with a nested regional climate model. *J. Clim.* **7** 375-399.

GORDON HB (1981) A flux formulation of the spectral atmospheric equations suitable for use in long-term climate modelling. *Mon. Weather. Rev*. **109** 56-64.

GORDON HB (1983) Synoptic cloud variations in a low resolution spectral atmospheric model. *J. Geophys. Res.* **88** 6563-6575.

GORDON HB and O'FARRELL SP (1997) Transient climate change in the CSIRO global coupled model with dynamical sea ice. *Mon. Weather. Rev.* **125** 875-907.

JACKSON SP (1954) Sea breezes in South Africa. *SA Geogr. J.* **36** 13-23.

JENKINS GS and BARRON EJ (1997) Global climate model and coupled regional climate model simulations over the eastern United States: GENESIS and RegCM2 simulations. *Global and Planetary Change* **15** 3-32.

JOUBERT AM (1997) Simulations by the Atmospheric Model Intercomparison Project of atmospheric circulation over Southern Africa. *Int. J. Climatol.* **17** 1129-1154.

JOUBERT AM, KATZFEY JJ, McGREGOR JL and NGUYEN KC (1999) Simulating mid-summer climate over southern Africa using a nested regional climate model. *J. Geophys. Res.* **104** 19015-19025.

KALNAY E et al. (1996) The NCEP/NCAR 40-year reanalysis Project. *Bull Amer. Meteorol. Soc.* **77** 437-472.

KONDO J, SAIGUSA N and SATO T (1990) A parameterisation of the evaporation from bare soil surfaces. *J. Appl. Meteorol.* **29** 385-389.

LOUIS JF (1979) A parametric model of vertical eddy fluxes in the atmosphere. *Bound.-Layer Meteorol.*, **17** 187-202.

McGREGOR JL and WALSH K (1991) *Summertime climate simulations for the Australian region using a nested model*. Proc. 5th Conf. on Climate Variations, Denver, CO. Amer. Meteorol. Soc., 515-518.

McGREGOR JL and WALSH K (1993) Nested simulations of perpetual January climate over the Australian region. *J. Geophys. Res*. **98** 23283-23290.

McGREGOR JL, WALSH KJ and KATZFEY JJ (1993a) *Nested modelling for regional climate studies*. In: Jakeman AJ Beck MB McAleer MJ (eds.) *Modelling Change in Environmental Systems.* Chichester: John Wiley, pp. 367-386.

McGREGOR JL, GORDON HB, WATTERSON IG, DIX MR and ROTSTAYN LD (1993b) *The CSIRO 9-level Atmospheric General Circulation Model.* CSIRO Division of Atmospheric Research Technical Paper No. **26**, Aspendale, Vic, Australia. 89 pp.

McGREGOR JL and WALSH K (1994) Climate change simulations of Tasmanian precipitation using multiple nesting. *J. Geophys. Res.* **99** 20889-20905.

McGREGOR JL (1997) Regional climate modelling. *Meteorol. Atmos. Phys.* **63** 105-117.

McGREGOR JL (1999) *Regional Modelling at CAR: Recent Developments*. BMRC Report No **75** 43-48.

NEW M, HULME M and JONES P (1999) Representing twentieth-century space-time climate variability. Part I: Development of a 1961-90 mean monthly terrestrial climatology. *J. Clim.* **12** 829-856.

RAUTENBACH CJ deW (1999) Introduction of a Hybrid Vertical Co-Ordinate to An Atmospheric General Circulation Model. Ph.D.-thesis, University of Pretoria, 149 pp.

SCHWARZKOPF MD and FELS SB (1991) The simplified exchange method revisited: an accurate, rapid method for computation of infrared cooling rates and fluxes. *J. Geophys. Res.* **96** 9075-9096.

WALSH K and McGREGOR JL (1995) January and July climate simulations over the Australian region using a limited area model. *J. Clim.* **8** 2387-2403.